A NEW APPARATUS FOR COMPRESSION TESTING OF WOOD[1]

Jozsef Bodig
Department of Forest and Wood Sciences, Colorado State University, Fort Collins
and
James R. Goodman
Department of Civil Engineering, Colorado State University, Fort Collins

ABSTRACT

Discussion is presented concerning the nature of stress distribution in a compression block. Two major factors, the mismanufacturing of specimens and the misalignment in respect to the center of the loading axis, are shown to be the major causes of eccentric loading in compression. The authors have desiged a new compression apparatus which was proved by both theoretical consideration and by experimental data to be better than the presently used single spherical bearing block. Using two spherical bearing blocks reduces considerably the undesirable side effects in comparison to the one spherical block system, but neither of these two techniques is designed for accurate specimen centering. The effect of the three loading systems in creating distortion in a compression specimen was evaluated. Six basic measured strain properties proved to be affected by these testing techniques.

INTRODUCTION

During the course of a research study on the orthotropic elastic parameters of wood in compression, the authors encountered some difficulty in reproducing accurate values, especially some of the Poisson's ratios, by using the ASTM standard testing method for compression parallel to grain (ASTM 1965). It was felt that the irregularity of values was more than could be attributed to the inherent natural variation in wood, and a small study was originated to evaluate the stress conditions existing in a block of wood in compression. This paper reports on the findings of this study.

While it is difficult to find literature which explains the reasons for the introduction of the spherical bearing block into compression testing, the need for its use most likely arose from the problem of manufacturing perfect contact surfaces. Consequently the ASTM standard (1965) used today for compression of wood requires the use of at least one spherical bearing block as shown in Fig. 1. This spherical bearing block probably was designed to take care of specimen mismanufacturing. There is no arrangement, however, to insure correct centering of the blocks, over the spherical block. This lack of accurate centering, combined with sample manufacturing errors, will cause deviation from a uniformly distributed compression stress as will be demonstrated.

It is a well-known fact that pure compression is not attained at the specimen-compression head interface because of the frictional forces developed there (Bodig 1966; Kobayashi 1962). It is generally assumed, however, that at a certain distance away from loading interfaces, uniform compression stresses are attained (Ellwood 1954). How far one actually has to move away from the interfaces to attain only compression stress is a matter of judgment at the present at least for testing wood. The authors are currently investigating this problem by finite element techniques.

ANALYSIS OF BEARING SYSTEMS

Assume, for the time being, that the specimens can be perfectly centered, but that the surfaces which are loaded are nonparallel. Nonparallel surfaces are those

[1] The authors wish to express their appreciation to the National Science Foundation for providing funds to study the "Orthotropic Elastic and Strength Properties of Wood" (Grant GK-1877). This report is a part of this study.

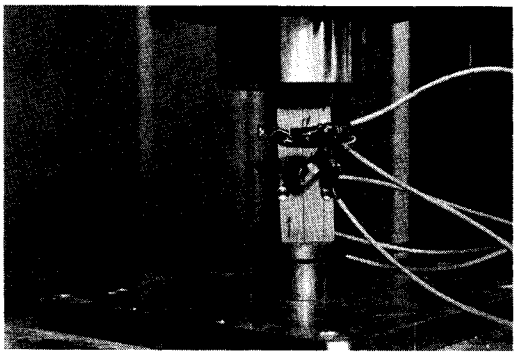

FIG. 1. Compression test setup with one spherical compression plate.

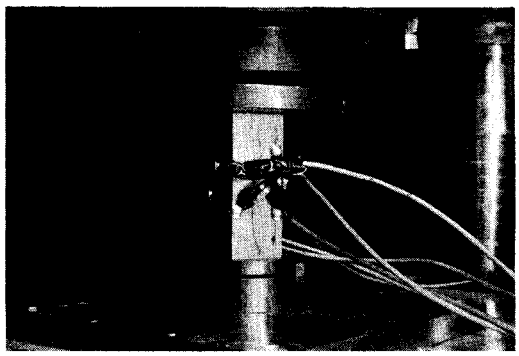

FIG. 3. Compression test setup with two spherical compression plates.

which converge, as shown with specimens "A" in Fig. 2. In addition, parallel but nonrectangular cuts are possible as well, as shown by specimens "B."

Conditions IA and IB in Fig. 2 illustrate what happens if one spherical block is used for specimen with the assumed cutting errors. The steps involved in the compression testing are as follows: 1) the specimen is centered on the base of the testing machine; 2) it comes into contact with the spherical bearing block; and 3) finally the bearing block realigns itself for complete surface contact. This final arrangement is shown in each of the parts of Fig. 2. As can be seen

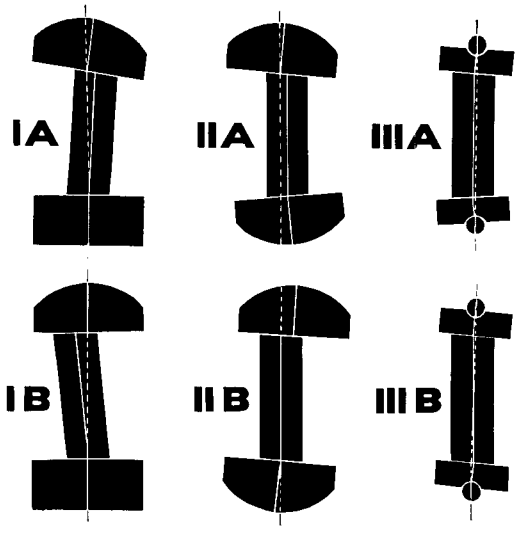

FIG. 2. Misalignment of compression specimens with three different testing apparatus.

by the difference between the solid line (center of the specimen) and the dotted line (center of the loading axis) on the specimens, a considerable angle of loading is introduced by using only one spherical block. Of course with perfect specimen manufacturing, the only error would be in the inaccuracy of centering. With perfect specimens no spherical bearing block would be necessary.

The situation considerably improves, especially for condition "B," with the use of two spherical loading heads. The angle of loading here changes to a direct eccentric loading, causing bending of specimen IIA. Condition IIB is ideal for the assumed case of two perfectly parallel but nonrectangular surfaces. Fig. 3 shows such a mismanufactured specimen being loaded by two spherical compression heads.

The magnitude of eccentricity induced in compression for a given cut is proportional to the radius and thickness of the spherical bearing blocks. From this consideration, the authors decided to change the design of the bearing block for compression testing. The ideal design would be a pin-point support at both ends of the specimen with infinitely thin plates for uniform load distribution. Of course this ideal condition cannot be attained with finite specimen dimensions, and a certain compromise must be built into the system. The revised apparatus (see Figs. 2 IIIA, IIIB, and 4) consists of a supporting plate at each end of the specimen, and each plate is loaded through a

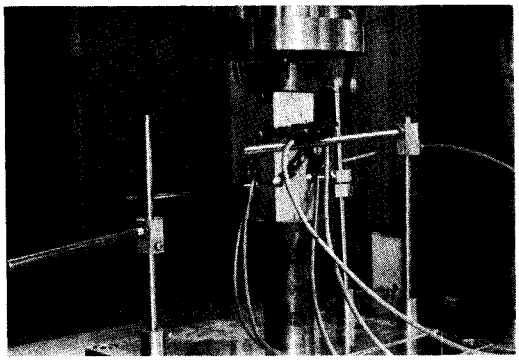

FIG. 4. Compression test setup with ball bearings.

partially embedded ball bearing. Centering pins are built into the supporting plates (Fig. 4) to permit accurate specimen centering. As has been stated previously, this arrangement does not completely eliminate eccentricity or inclined loading, but it reduces these effects relative to the presently used techniques as illustrated in Fig. 2. Data based on the results of experiments designed to verify the theoretical predictions already outlined are presented below.

EXPERIMENTAL VERIFICATION

A small study with a limited number of specimens was set up to underline the validity of the predicted stress distributions. Only a small number of samples were selected for the study since the authors were not seeking an exact comparison of values between the three different techniques, shown in Fig. 2, but rather a comparison of the relative performance of these systems.

For this experimental study, 18 compression specimens of 1¾ inch by 1¾ inch cross sections and 5 inches high were prepared from a single piece of air-dry redwood lumber, with all defect-free specimens from the same annual ring locations. For each of the six conditions shown in Fig. 2, three samples were selected randomly and tested in compression parallel to the grain.

Electrical resistance strain gauges were used on the clip gauges shown in Figs. 1, 3 and 4 to measure the strains on the front and back faces of the specimens.

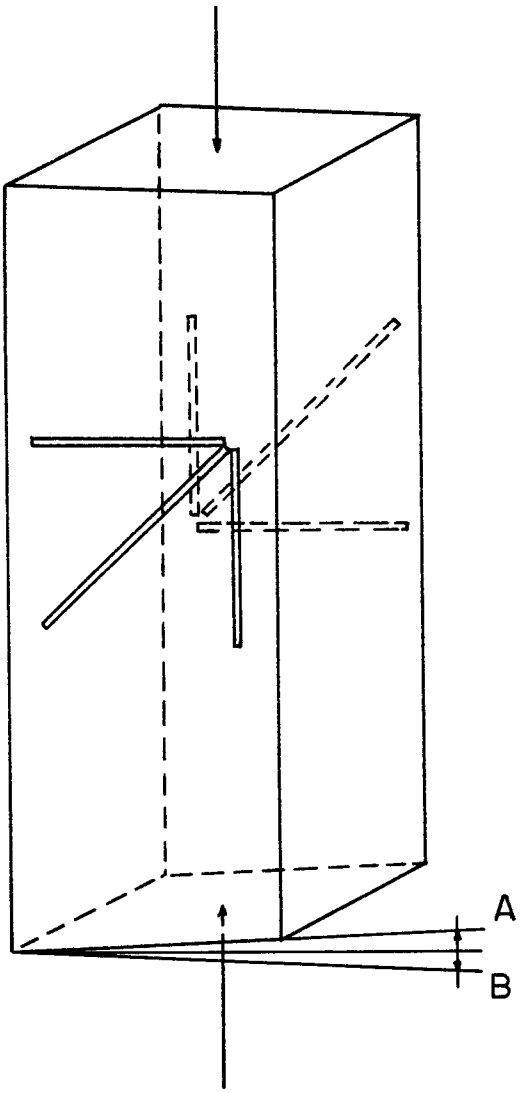

FIG. 5. Locations of clip-gauges on a compression test specimen.

These gauges were arranged parallel, 45 degrees, and perpendicular to the axis of load (Fig. 5) permitting the computation of shear deformations (Stieda 1968). Each strain gauge output was automatically recorded on strip chart recorders. Letters A and B on Fig. 5 designate the angle of cut for the types of specimens tested.

Deformation data were taken from each chart at 15-second intervals, and the various strain conditions were computed. The shear

TABLE 1. *Test results of various properties evaluated after one minute of testing.*

Method	I		II		III		All	
Specimen / Replication	A	B	A	B	A	B	A	B
	"1" $(\epsilon_{front} - \epsilon_{back}) \cdot 10^6$ in./in.							
1	−1388	−912	−1790	+190	−135	−142		
2	−2122	−784	−906	+78	−234	−360		
3	−1532	+833	−247	−328	+747	+239		
$\bar{x}$ abs	1681	842	981	199	372	247	1011	429
s	388.9	65.5	774.2	125.2	328.5	109.2		
$\bar{x}$ abs	1262		590		310		720	
	522.6		655.5		229.4			
	"2" $(\gamma_{ave}) \cdot 10^6$ radian							
1	+45	+61	+357	−258	−79	−189		
2	+338	+33	−64	−179	+13	−233		
3	+392	−1288	−205	−355	−508	−396		
$\bar{x}$ abs	258	461	208	264	200	273	222	332
s	186.7	716.6	146.5	88.2	268.8	109.0		
$\bar{x}$ abs	360		236		236		277	
s	481.3		112.3		187.7			
	"3" $(\gamma_{f.abs} - \gamma_{b.abs}) \cdot 10^6$ radian							
1	585	797	744	517	252	378		
2	1234	434	1144	358	147	465		
3	1231	2576	1795	711	1017	793		
$\bar{x}$ abs	1047	1269	1228	529	472	545	915	781
s	402.2	1146.4	530.5	176.8	474.9	218.9		
$\bar{x}$ abs	1158		878		509		848	
s	777.9		521.2		333.1			
	"4" $(\gamma_{f.abs} - \gamma_{b.abs})$ $(\gamma_{ave.abs})$ radian^2							
1	25	49	256	133	20	71		
2	418	14	73	64	19	106		
3	518	3315	369	252	517	314		
$\bar{x}$ abs	320	1126	242	150	185	164	249	480
s	260.6	1895.8	162.0	95.1	287.2	131.4		
$\bar{x}$ abs	723		196		174.5		364	
s	1288.2		129.0		200.1			
	"5" T_f (sec.)							
1	195	270	165	165	270	270		
2	225	225	240	240	255	225		
3	240	240	195	240	255	285		
$\bar{x}$	220	205	200	215	260	260	227	227
s	22.9	48.2	37.7	43.3	8.7	31.2		
$\bar{x}$	2130		208		260		227	
s	34.8		37.3		30.5			

TABLE 1. *(Continued)*

Method	I		II		III		All	
Specimen / Replication	A	B	A	B	A	B	A	B
	"6" T_t (sec.)							
1	20	24	24	20	24	24		
2	48	10	20	21	17	20		
3	37	40	24	17	15	26		
$\bar{x}$	35	25	23	19	19	23	25	22
s	14.1	15.0	2.3	2.1	4.7	3.1		
$\bar{x}$	30		21		21		24	
s	14.2		2.7		4.4			

strain (γ) is computed, utilizing Mohr's circle from the equation:

$$\gamma = \frac{2\frac{\Delta_2}{L_2} - \left(\frac{\Delta_1}{L_1} + \frac{\Delta_3}{L_3}\right)}{2}$$

where Δ_1, Δ_2, and Δ_3 are the vertical, diagonal, and horizontal deformations and L_1, L_2, and L_3 are the corresponding gauge lengths.

From the deformation measurements and the force-time curve recorded on a 50,000 lb Instron testing machine, the following properties were computed:

E_L = modulus of elasticity along the grain
$\epsilon_f - \epsilon_b$ = axial strain difference between the front and back face
γ_{ave} = average shear strain
$\gamma_{f.abs} - \gamma_{b.abs}$ = absolute shear strain difference between the front and back face
$(\gamma_{f.abs} - \gamma_{b.abs})\gamma_{ave}$ = weighed shear strain difference
T_f = time from the start of the test to failure
T_t = time from the start to tangent zero load
σ_{max} = max compression stress

RESULTS

For each of the above-mentioned properties a two-way analysis of variance was run to evaluate the significance of each test and specimen type. Modulus of elasticity, E_L, did not prove to be significantly affected by the type of test, although the axial strain differences between the front and back faces were significantly affected. For the modulus of elasticity computation, the bending effect was eliminated by using the average axial strain, which explains its nonsignificance. The other property which did not prove to be significantly affected by the tests was the maximum compression stress, σ_{max}. The other properties listed all proved to be significantly affected at least at the 10% level.

Table 1 shows that the axial strain difference ($\epsilon_f - \epsilon_b$) was the highest for method I (one spherical block), 0.001262 in/in less for method II (two spherical blocks) 0.000590 in/in, and the smallest for method III (new apparatus) 0.000310 in/in. Also specimen A had a larger difference 0.0001000 in/in than specimen B, 0.000429. The smallest difference occurred with condition IIB, 0.000199 which follows exactly the predictions made above under Analysis of Bearing Systems.

The average shear strain did not prove to be a good indicator of the true shear condition of the system. Often shear strain assumed different directions in the front and back faces and their average did not indicate the actual condition. They are nevertheless included in Table 1 for observation. Fig. 6 shows this to be true for condition II where the average shear strain was close to zero, yet large shear strains were present on both the front and back

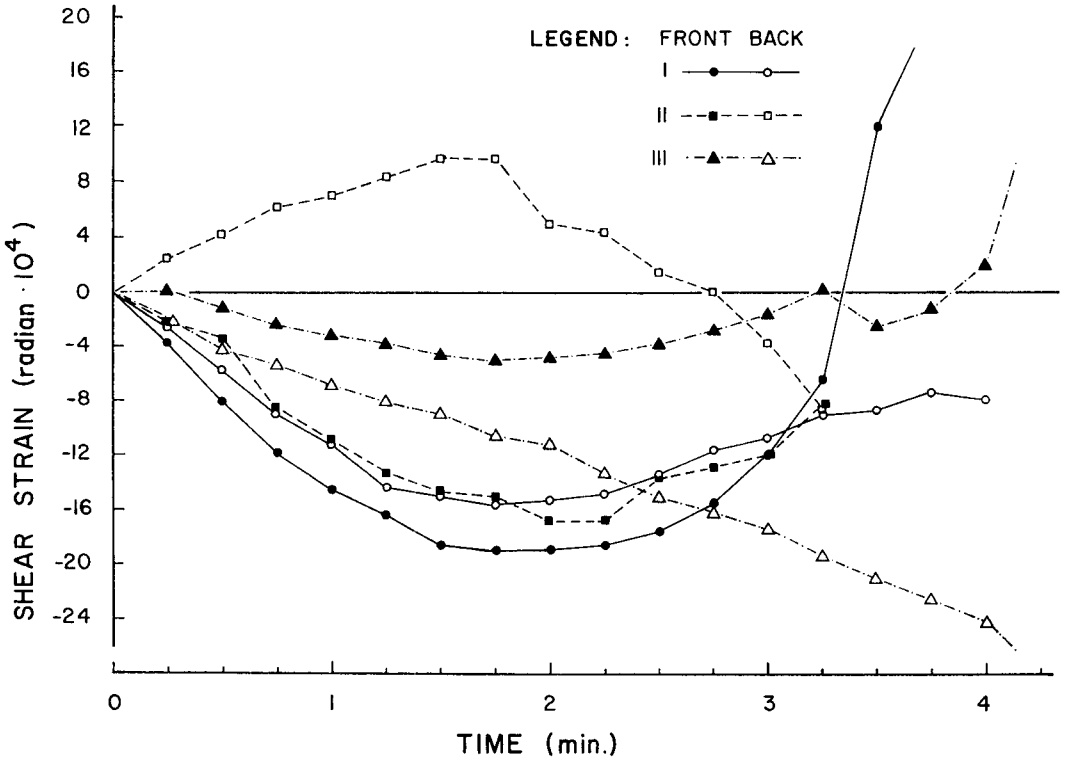

FIG. 6. Shear strain development in compression on selected specimens.

faces. The difference between the absolute shear strain values ($\gamma_{f.abs} - \gamma_{b.abs}$) somewhat better indicated the presence of shear but sometimes proved to be just as much of a problem as the average shear strain as indicated in Table 1.

Further attempts were made to find a parameter which expresses both the magnitude and difference between the shear strains of the front and back faces. The weighted shear strain difference $(\gamma_{f.abs} - \gamma_{b.abs})\gamma_{ave}$ was finally computed. While this parameter considerably better expresses the shear condition than the previous two, the axial strain difference also has to be considered to visualize the complete distortion. Fig. 6 shows plots of shear strain versus time for the case of the largest value of weighted shear strain difference for each of the three testing problems as a function of testing time.

The magnitude of shear strain was considerably less, as shown in Table 1, for the new testing technique than those of the other two testing methods. The irregular shape of the shear strain-time curve beyond 1¾ minutes (Fig. 6) is due to the stress conditions beyond the proportional limit and is of no value in the determination of elastic parameters.

Fig. 7 shows typical stress-loading time curves for each of the testing techniques. These curves were obtained from the recorded load versus head movement curves. The curves in Fig. 7 are included in this report to show the general stress-loading time relationship. This figure illustrates also how time to failure has been increased for the new testing method. This increase in failure time can be explained by the reduced distortion and bending effect. The time in seconds, T_t, between the starting of the stress application and the maximum slope tangent line at zero stress (Fig. 7) also proved to be different for the three methods of testing. Methods II and III required less

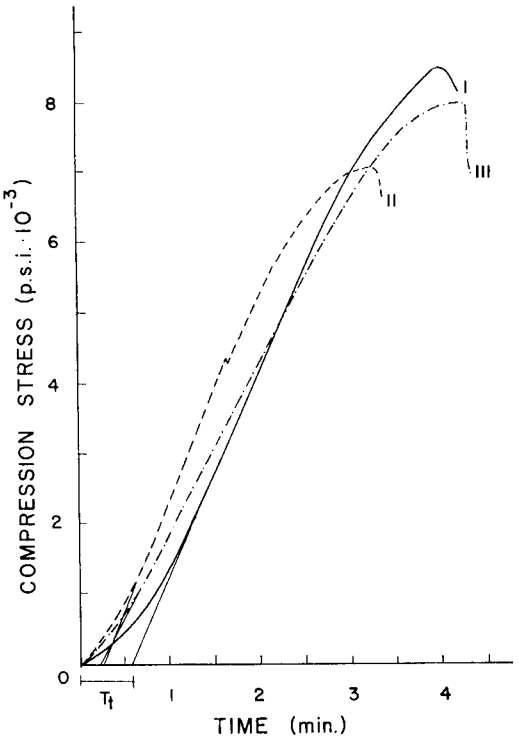

FIG. 7. Stress-time curves for selected specimen measured on total specimen height.

time to attain linearity than method I (Table 1). This property again illustrates the problems associated with the use of one spherical block.

The data in Table 1 were analyzed further to establish significant differences between the various testing techniques and specimen shapes. Table 2 shows the result of the "t" tests. Because of the small sample size and the available theoretical predictions, the 10% probability level was accepted as the basis of significant difference. The difference between two variables was accepted if either the variance or the mean proved to be significant.

Table 2 shows the meaningful interactions between test methods and specimen types which result from "t" tests for the six properties listed in Table 1. From the theoretical consideration, significant differences are predicted (shaded areas) between methods IA–IIIA, IB–IIB, IB–IIIB, IIA–IIB, and IIA–IIIA. Table 2 shows that in 19 out of 30 cases, significant differences were established even with the limited sample size. Significance was nearly always found for the axial strain difference, which is one of the most important factors in evaluating the presence of bending stresses on the compression specimens.

By combining specimens A and B, the effect of testing apparatus alone can be evaluated as shown in Table 3. The significant improvement between techniques I and II is quite convincing, and the differences are even more pronounced between techniques I and III. The difference is not so large when techniques II and III are considered. The significances shown in Tables 2 and 3 have to be combined with the mean and standard deviation values presented in Table I to make meaningful comparisons with the theoretical predictions.

CONCLUSIONS

From the presented data, it can be concluded that considerable eccentricity is present on the bending specimens using the presently accepted testing technique utilizing one spherical compression head. The introduction of an additional spherical compression head considerably reduces the undesirable effects of bending and shear. The new apparatus, applied here, reduces the shear strain to about one-fourth of that obtained with one spherical block.

The spherical arrangement partially solves the problem of specimen mismanufacturing, but it does not take into consideration the problem caused by imperfect specimen centering. Accurate specimen centering especially with the ball-bearing arrangement is a necessity if one is to reduce the error caused by the assumption of the presence of perfect uniform compression stress in the area where measurements are taken. The use of one single spherical block in compression testing is strongly discouraged in favor of the new ball-bearing arrangement or the use of two spherical blocks with the addition of some centering device.

TABLE 2. *Summary of "t" test results in comparing testing methods and specimen shapes*

Method	Specimen	Property[1]	I		II		III
			A	B	A	B	A
I	B	1	**				
		2	*				
		3	N.S.				
		4	**				
		5	N.S.				
		6	N.S.				
II	A	1	N.S.				
		2	N.S.				
		3	N.S.				
		4	N.S.				
		5	N.S.				
		6	**				
	B	1		****	**		
		2		**	N.S.		
		3		**	**		
		4		***	N.S.		
		5		N.S.	N.S.		
		6		**	*		
III	A	1	****		N.S.		
		2	N.S.		N.S.		
		3	*		*		
		4	N.S.		N.S.		
		5	**		**		
		6	N.S.		N.S.		
	B	1		****		N.S.	N.S.
		2		**		N.S.	N.S.
		3		**		N.S.	N.S.
		4		***		N.S.	N.S.
		5		*		N.S.	N.S.
		6		**		*	N.S.

[1] Numbers correspond to properties numbered in Table 1.
N.S. = nonsignificant at 10% probability level
* significant at 10% probability level
** significant at 5% probability level
*** significant at 1% probability level
**** significant at 0.1% probability level

TABLE 3. *Summary of "t" test results in comparing testing techniques*

Method	Property	I	II
II	1	**	
	2	***	
	3	*	
	4	***	
	5	N.S.	
	6	***	
III	1	**	**
	2	**	N.S.
	3	**	**
	4	***	N.S.
	5	***	***
	6	**	N.S.

For notation see Table II

REFERENCES

AMERICAN SOCIETY FOR TESTING AND MATERIALS. 1965. Standard method of testing small clear specimens of timber. ASTM Designation D 143-52.

BODIG, J. 1966. Stress-strain relationship of wood in transverse compression. J. Materials **1**(3): 645–666.

ELLWOOD, E. L. 1954. Properties of American beech in tension and compression perpendicular to grain and their relation to drying. School of Forestry Bulletin No. 61, Yale University.

KOBAYASHI, S. 1962. Restraint in compression test of orthotropic materials. Forest Prod. J. **12**(10): 489–492.

STIEDA, C. K. A. 1968. Computer evaluation of strain gage rosette readings. Instrument & Control Systems **41**(11): 73–74.